

Synthesis of In₂O₃/Carbon Core-Shell Nanospheres and their Electrochemical Performance

Jie Liu¹, Yongchun Zhu^{1,*}, Jianwen Liang¹ and Yitai Qian^{1,2,*}

¹ Hefei National Laboratory for Physical Science at Microscale and Department of Chemistry, University of Science and Technology of China, Hefei, Anhui 230026, PR China

² School of Chemistry and Chemical Engineering, Shandong University, Jinan 250100, PR China

*E-mail: ytqian@ustc.edu.cn; liujie01@mail.ustc.edu.cn.

Received: 20 April 2012 / Accepted: 17 May 2012 / Published: 1 June 2012

In₂O₃/C core-shell nanospheres have been synthesized via template-free hydrothermal approach at 200 °C first, then treated in glucose aqueous solution and annealed at 500 °C. The products were around 100 nm in dimension with carbon shell about 10 nm in thickness. Electrochemical tests demonstrated that the In₂O₃/C core-shell nanospheres had an initial discharge capacity as high as 1607 mAh g⁻¹ and the discharge capacity of 569 mAh g⁻¹ after 50 cycles at 0.1 C. Moreover, the products showed the discharge capacities of 578, 361, 279, 173 mAh g⁻¹ at the rates of 0.1, 0.2, 0.5 and 1 C, respectively.

Keywords: Hydrothermal / Indium Oxide / Core-shell / Electrochemical.

1. INTRODUCTION

The core-shell nanostructure is now attracting more and more investigation interest for its wide potential applications in fuel cell[1], lithium-ion battery[2], catalytic synthesis[3], owing to its combination of the functions of both the core and the shell[4]. A series of core-shell nanostructures, including double-shelled coaxial nanocables[5], nanoparticles[6], nanowires[7], nanotubes[8] and hollow spheres[9] have been synthesized. Among these core-shell structures, carbon coating structures provide a useful strategy to improve the electrochemical performance of active materials with high electronic conductivity, good lithium permeability and flexible accommodation of volume change[10].

Indium oxide (In₂O₃), an important n-type transparent semiconductor with wide band gap (3.5-3.75 eV)[11], high optical transparency[12], high electrical conductivity[13], and excellent luminescence[14] has received enormous interest for its extensive applications in optoelectronic

devices[15], transistors[16], solar cells[17], gas sensors[18] and electrode materials in lithium ion battery[19-21].

Since indium oxide nanobelts were reported in 2001[22], various kinds of In_2O_3 nanostructures, such as quasi-monodisperse In_2O_3 nanoparticles[23], nanowires[24], nanotubes[25], nanocubes[26], In_2O_3 octahedrons[27] and core-shell In_2O_3 nanoparticles[6] have been prepared via various methods. The core-shell In_2O_3 nanocomposites have been usually synthesized by solid-state reaction[28], physical vapor deposition[7], radio frequency sputtering technique[5].

Considering the large theoretical specific capacity of In_2O_3 [21], electrochemical properties on In_2O_3 have been reported successively. For instance, nanostructured In_2O_3 thin films prepared by pulsed laser deposition method exhibited a large capacity of 1083 mAh g^{-1} in the first discharge, however, the capacity dropped to 504 mAh g^{-1} after 30 cycles[19]. By cathodic electrochemical synthesis in aqueous solution, the obtained In_2O_3 films, which were formed by agglomerate nanoparticles, delivered a discharge capacity of 1400 mAh g^{-1} in the first cycle and maintained a stable and reversible capacity of 195 mAh g^{-1} after 10 cycles between 0.2 and 1.2 V[20].

Herein, to synthesize the $\text{In}_2\text{O}_3/\text{C}$ core-shell nanospheres, we use a template-free hydrothermal approach in the polyethylene glycol (PEG) 400 system at $200 \text{ }^\circ\text{C}$ for 24 h first, then treated in glucose aqueous solution and annealed at $500 \text{ }^\circ\text{C}$ for 3 h. Electrochemical performance of $\text{In}_2\text{O}_3/\text{C}$ core-shell nanospheres showed the discharge capacities of 1607 mAh g^{-1} in the first cycle and 569 mAh g^{-1} in the fiftieth cycle, which exhibited improved cycling behavior performance and an obvious enhancement in discharge capacity compared with the electrochemical properties of In_2O_3 ever reported[19-21].

2. EXPERIMENTAL

2.1 Synthesis.

All the reagents in analytic grade were purchased from Shanghai Chemical Reagents Co. and were used as-received without further purification. In a typical experimental synthesis, 1 mmol of $\text{In}(\text{NO}_3)_3 \cdot 4.5\text{H}_2\text{O}$ and 0.5 g of $\text{CO}(\text{NH}_2)_2$ were dissolved in 40 mL of PEG 400 under stirring. Then, 1 mL of distilled H_2O , 1.5 mL of $\text{NH}_3 \cdot \text{H}_2\text{O}$ (25 wt%), and 4.5 mL of concentrated HNO_3 were added to the above solution. The mixture was stirred until it became homogeneous and then was sealed in a Teflon-lined stainless steel autoclave (60 mL capacity). The autoclave was maintained in an oven at $200 \text{ }^\circ\text{C}$ for 24 h. The raw products were washed with distilled H_2O and anhydrous ethanol for several times to remove ions and possible remnants, and finally dried in a vacuum chamber at $60 \text{ }^\circ\text{C}$ for 6 h. The brown solid precursors were obtained. Then treated in glucose aqueous solution, dried in the vacuum chamber at $60 \text{ }^\circ\text{C}$ for 12 h, annealed at $500 \text{ }^\circ\text{C}$ for 3 h in argon atmosphere, the products were obtained.

2.2 Characterization.

The products were characterized by powder X-ray diffraction (XRD) performed on a Philips X'Pert diffractometer with $\text{Cu K}\alpha$ radiation ($\lambda = 1.54178 \text{ \AA}$). Scanning electron microscopy (SEM) images were taken on a JEOL JSM-6700F scanning electron microscope. Transmission electron

microscopy (TEM) images and high-resolution TEM (HRTEM) images were obtained on the JEOL-2010 transmission electron microscope operating at 200 kV. Raman spectrum was performed at room temperature with a LABRAM-HR laser spectrometer with an argon-ion laser at an excitation wavelength of 514.5 nm. The samples used for SEM, TEM and HRTEM characterization were dispersed in absolute ethanol and were slightly ultrasonicated before observation. The charge–discharge measurements were conducted on a Land CT 2001A automatic battery tester (Wuhan, China).

2.3 Electrochemical measurements.

The electrochemical performance was tested by using coin-type cells (CR2016) at room temperature. The working electrodes were made by mixing the products, acetylene black and polyvinylidene fluoride (PVDF) in N-methylpyrrolidone (NMP) at a weight ratio of 8:1:1. The resulting paste was uniformly coated onto a Cu foil and dried in the vacuum chamber at 100 °C for 10 h, before being cut into disks with a diameter of 8 mm. The coin-type cells were assembled in an glove box under argon atmosphere with the prepared disks as working electrodes, lithium metal as the counter electrodes, microporous membrane (Celgard 2300) as separators and 1M LiPF₆ mixed in a solution of ethylene carbonate (EC) and dimethyl carbonate (DMC) (1:1) in volume as electrolyte. The charge–discharge measurements were conducted on a Land CT 2001A automatic battery tester (Wuhan, China).

3. RESULTS AND DISCUSSION

3.1 Phase of the In₂O₃/C core-shell nanospheres.

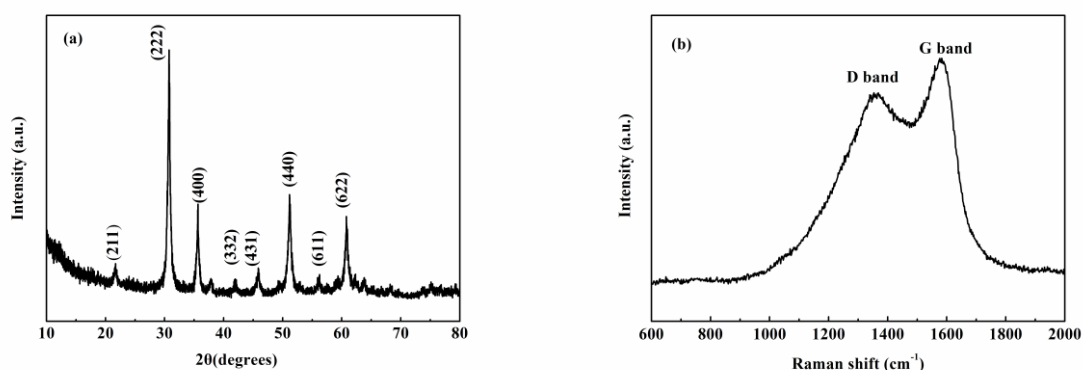


Figure 1. (a) XRD pattern (b) Raman spectrum of the products

Figure 1a shows the XRD pattern of the products. All the diffraction peaks can be also indexed as cubic In₂O₃ ($a_0 = 10.1170 \text{ \AA}$, space group: Ia3(206), JCPDS No. 71-2194). Raman spectrum was used to examine the shell composition of the obtained nanospheres. The Raman spectrum of the

products (Figure 1b) displays two strong peaks at 1353 and 1583 cm^{-1} , which can be assigned to the disordered amorphous carbon (D band) and graphic carbon (G band), respectively[29]. The ID/IG value of the sample is 0.89, indicating that the outer carbon shells of the obtained products possessed a mass of disorder and defects, according to a previous report[30].

3.2 Morphology of the $\text{In}_2\text{O}_3/\text{C}$ core-shell nanospheres.

Figure 2a provides a SEM overview image. It is clear that the products are nanospheres. Figure 2b is the TEM image of the products, in which the dark/light contrast indicates the presence of the structure of core-shell nanospheres. The nanospheres are around 100 nm in overall dimension and the shell thicknesses are around 10 nm . It is also found that the carbon-framework connects the core-shell nanospheres together. Figure 2c is a high-magnification TEM image of the products, which presents that the cores of the products are consisted of many agglomerate nanoparticles. Figure 2d shows a HRTEM image of the adjacent regions between the core and the shell. The lattice fringe spacing of the core is 0.295 nm , corresponding to the (222) plane of cubic In_2O_3 (JCPDS Card File No. 71-2194).

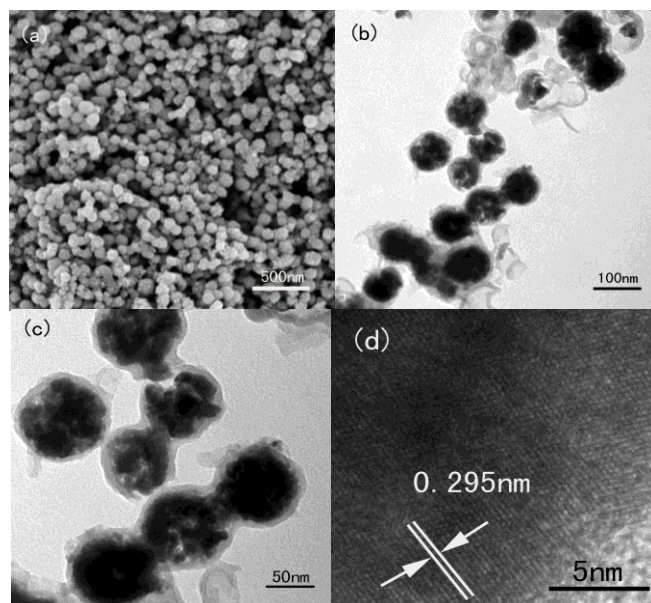


Figure 2. (a)SEM (b)TEM image and (c) high-magnification TEM image and (d) HRTEM image of the products.

3.3 Electrochemical performance of the $\text{In}_2\text{O}_3/\text{C}$ core-shell nanospheres.

To investigate electrochemical performance of the $\text{In}_2\text{O}_3/\text{C}$ core-shell nanospheres, the measurements of discharge capacity versus cycle number were carried out between 0.00V and 3.00V at the rate of 0.1 C . In the curve of Figure 3, it can be observed that the first discharge capacity of the $\text{In}_2\text{O}_3/\text{C}$ core-shell nanospheres is 1607 mAh g^{-1} , which corresponds to $16.7\text{ Li per In}_2\text{O}_3$ [19,21]. The second reversible capacity is found to be 1375 mAh g^{-1} , corresponding to $14.3\text{ Li per In}_2\text{O}_3$. The

capacity fade of the first cycle is about 14.4%. However, the capacity remains stable at about 575 mAh g⁻¹ after 20 cycles. After 50 cycles, the discharge capacity is still holding at 569 mAh g⁻¹, which indicates good coulombic efficiency and high specific capacities. It should be noticed that these values are higher than the capacities in the previous reports [19-21]. In Figure 4, the 10th, 20th, 30th, 40th, 50th discharge/charge curves of the In₂O₃/C core-shell nanospheres at 0.1C in the voltage of 0.00-3.00V present the charge-discharge potential plateaus which agree well with the previous report [19]. It can be also found that the discharge potential plateaus remain stable after 20 cycles, which corresponds to the results in Figure 3.

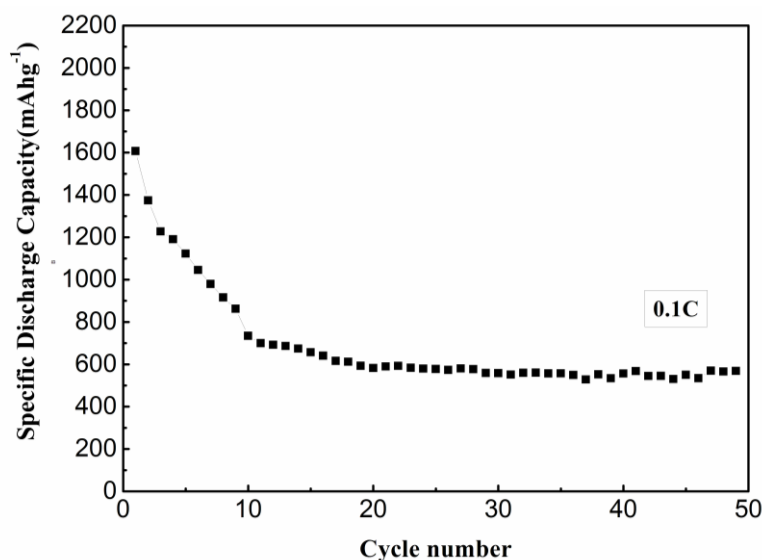


Figure 3. Profiles of the discharge capacity vs cycle numbers of the In₂O₃/C core-shell nanospheres.

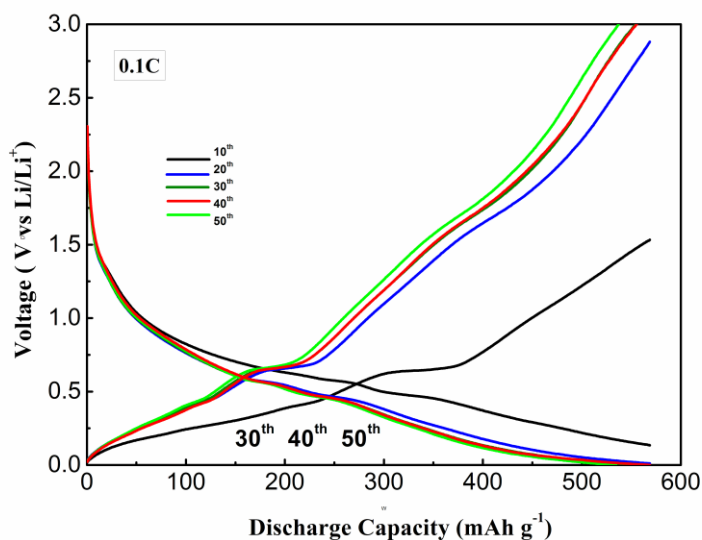


Figure 4. The charge-discharge curves of the In₂O₃/C core-shell nanospheres at the 10th, 20th, 30th, 40th, 50th at 0.1 C

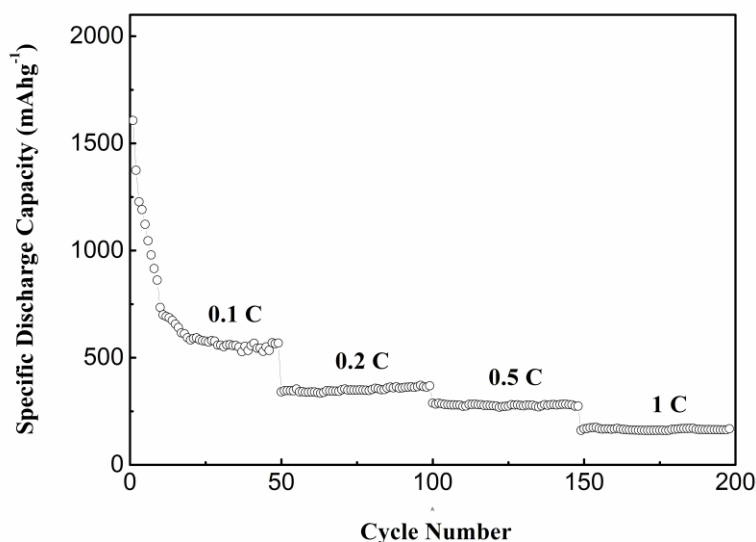


Figure 5. Discharge capacity curve vs cycle number of the $\text{In}_2\text{O}_3/\text{C}$ core-shell nanospheres at 0.1, 0.2, 0.5, 1C.

In Figure 5, the cycling performance of the $\text{In}_2\text{O}_3/\text{C}$ core-shell nanospheres were measured at different rates from 0.1 C to 1 C in an ascending order, for 50 cycles each. The discharge capacities maintain at around 578, 361, 279, 173 mAh g^{-1} at the rates of 0.1, 0.2, 0.5 and 1 C, respectively.

It can be found that both of the cycling behavior and discharge capacity have been greatly improved compared to the previous reports[19-21], which may be ascribed to the special core-shell nanostructure. First, the core-shell nanostructure provides enough contact areas for the electrode and electrolyte. Moreover, the carbon framework can buffer the volume change brought from the nanosized active materials on electrode and reduce the structure collapse of the active materials inside.

4. CONCLUSIONS

In summary, the $\text{In}_2\text{O}_3/\text{C}$ core-shell nanospheres were synthesized via one-step template-free hydrothermal approach at 200 °C, then further treated in glucose aqueous solution and annealed at 500 °C. The obtained $\text{In}_2\text{O}_3/\text{C}$ core-shell nanospheres are around 100 nm in size with carbon shells of 10 nm in thickness. Electrochemical performance of $\text{In}_2\text{O}_3/\text{C}$ core-shell nanospheres exhibited improved cycling behavior performance and enhanced discharge capacities compared with the electrochemical properties of In_2O_3 ever reported.

ACKNOWLEDGEMENTS

We thank the National Natural Science Fund of China (No. 91022033), the 973 Project of China (No. 2011CB935901) and the Fundamental Research Funds for the Central Universities (No. WK 2340000027).

References

1. Z.H. Wen, J. Liu, J.H. Li, *Adv Mater.* 20 (2008) 743.
2. Y. Yu, L. Gu, C. B. Zhu, P. A. van Aken, J. Maier, *J. Am. Chem. Soc.* 131(2009) 15984.
3. T. Harada, S. Ikeda, F. Hashimoto, T. Sakata, K. Ikeue, T. Torimoto, M. Matsumura. *Langmuir* 26(2010) 17720.
4. F. Caruso, *Adv. Mater.* 13(2001) 11.
5. H. G. Na, D. S. Kwak, H. W. Kim, *Cryst. Res. Technol.* 47(2012) 79.
6. Z.Y. Sun, A. Kumbhar, K. Sun, Q.S. Liu, J.Y. Fang, *Chem. Commun.* 16(2008) 1920.
7. C. W. Lai, J. Y. Dai, X. Y. Zhang, H. L. W. Chan, Y. M. Xu, Q. Li, H. C. Ong, *J. Cryst. Growth* 282(2005) 383.
8. H.K. Zhang, H.H. Song, X.H. Chen, J.S. Zhou, H.J. Zhang, *Electrochim. Acta* 59(2012) 160.
9. J. Liu, W. Li, A. Manthiram, *Chem. Commun.* 46(2010) 1437.
10. J. Liu, G.L. Yang, X.F. Zhang, J.W. Wang, R.S. Wang, *J. Power Sources* 197(2012) 253.
11. I. Hamberg, C.G. Granqvist, K.F. Berggren, B.E. Sernelius, L. Engström, *Phys. Rev. B* 30(1984) 3240.
12. Z. M. Jarzebski, *Phys. Status Solidi. A* 71(1982) 13.
13. S. Ishibashi, Y. Higuchi, Y. Oa, K. Nakamura, *J. Vac. Sci. Technol. A* 8(1990) 1399.
14. S. Park, C. Jin, H. W. Kim, C. Lee, *J. Alloys Compd.* 509(2011) 6262.
15. D. S. Ginley, C. Bright, *Mater. Res. Soc. Bull.* 25(2000) 15.
16. O. M. Berengue, A. J. Chiquito, L. P. Pozzi, A. J. C. Lanfredi, E. R. Leite, *Nanotechnology* 20(2009) 245706.
17. A. J. Miller, R. A. Hatton, G. Y. Chen, S. R. P. Silva, *Appl. Phys. Lett.* 90(2007) 023105.
18. G. Neri, A. Bonavita, G. Licali, G. Rizzo, N. Pinna, M. Niederberger, *Sens. Actuators B* 127(2007) 455.
19. Y.N. Zhou, H. Zhang, M.Z. Xue, C.L. Wu, X.J. Wu, Z.W. Fu, *J. Power Sources* 162(2006) 1373.
20. W.-H. Ho, C.-F. Li, H.-C. Liu, S.-K. Yen, *J. Power Sources* 175(2008) 897.
21. H. Li, X.J. Huang, L.Q. Chen, *Solid State Ionics* 123(1999) 189.
22. Z.W. Pan, Z.R. Dai, Z.L. Wang, *Science* 291(2001) 1947.
23. Q.S. Liu, Lu, W.G. A.H. Ma, J.K. Tang, J. Lin, J.Y. Fang, *J. Am. Chem. Soc.* 127(2005) 5276.
24. D.H. Zhang, C. Li, S. Han, X.L. Liu, T. Tang, W. Jin, C.W. Zhou, *Appl. Phys. Lett.* 82(2003) 112.
25. B. Cheng, E.T. Samulski, *J. Mater. Chem.* 11(2001) 2901.
26. Q. Tang, W.J. Zhou, W. Zhang, S.M. Ou, K. Jiang, W.C. Yu, Y.T. Qian, *Cryst. Growth Des.* 5(2005) 147.
27. H.B. Jia, Y.H. Zhang, X.H. Chen, J. Shu, X.H. Luo, Z.S. Zhang, D.P. Yu, *Appl. Phys. Lett.* 82(2003) 4146.
28. W.K. Chang, K. K. Rao, H.C. Kuo, J.F. Cai, M.S. Wong, *Appl. Catal A* 321(2007) 1.
29. T. Mei, T. Li, H. Y. Bi, L. B. Wang, Y. C. Zhu, Y. T. Qian, *Eur. J. Inorg. Chem.* 27(2010) 4314.
30. W.Z. Wang, L. Sun, Z. Fang, L.Y. Chen, Z.D. Zhang, *Cryst. Growth Des.* 9(2009) 2117.